

HYPERVELOCITY IMPACT EXPERIMENTS IMPLICATE IMPACT MELT AS A HOST FOR IMPACT-DELIVERED WATER ON ASTEROIDS. R. T. Daly¹ and P. H. Schultz¹, ¹Department of Earth, Environmental and Planetary Sciences, Brown University, 324 Brook St., Box 1846, Providence, RI, 02912; terik_daly@brown.edu.

Introduction: Impacts ferried water (including OH in hydrous minerals) from beyond the snow line to the inner solar system during planet formation [1]. Similar processes operate today. Evidence for impact-delivered water comes in many forms: exogenic, H- and OH-rich material on Vesta [2–4], hydrated carbonaceous chondrite clasts and microclasts in meteorites [5–8], and polar volatiles on the Moon and Mercury [9,10]. Shock physics codes also document water delivery from asteroids and comets to moons and planets [11–13].

Nevertheless, shock physics codes cannot yet fully represent material behavior (e.g., vaporization), particularly at lower impact speeds (e.g., $\sim 5 \text{ km s}^{-1}$) [14]. However, such speeds typify the main asteroid belt [15]. Shock physics codes also have a limited capacity to assess projectile-target interactions [e.g., 16]. Hypervelocity impact experiments can fill these gaps. Experiments are not limited by how well equations of state or constitutive relationships are implemented. Experiments incorporate projectile-target interactions down to the micron scale, thereby capturing detailed processes that shock physics models currently cannot resolve. Hence, experiments reveal information that shock physics codes currently cannot provide.

This study uses hypervelocity impact experiments to measure how efficiently impacts deliver water. Though limited in speed and size, these experiments measure the amount of water delivered by impact, interrogate how that water is stored (e.g., hydrous melts vs. projectile relics), assess speciation (OH vs. H_2O), and explore the distribution of delivered water.

Methods: Experiments were performed at the NASA Ames Vertical Gun Range [17]. The AVGR features a large impact chamber that allows volatiles liberated by impact to freely expand. AVGR experiments can match the single shock loading path of natural impacts. This generates higher post-shock temperatures than ring up experiments and may enhance devolatilization [18]. The AVGR also allows launching projectiles at a variety of angles, which introduces free-surface effects and frictional shear heating [19]. Hence, the AVGR is well-suited for studying devolatilization and, by extension, volatile delivery.

Two types of experiments were conducted for this study: “hydrous projectile” and “hydrous target”. While preliminary experiments were reported by [20,21], the present study is more comprehensive. In hydrous projectile experiments, serpentine projectiles ($\sim 12 \text{ wt.}\% \text{ OH}$) were fired into dry powdered pumice or sand. In

hydrous target experiments, water-poor Pyrex projectiles were fired into powdered serpentine. This strategy assessed differences in the water contents of materials created when water is delivered by the projectile vs. liberated from the target. Impact angle ranged from 30° to 90° ; impact speed was $\sim 5 \text{ km s}^{-1}$, comparable to main belt impact speeds [15]. Hence, impact speed need not to be scaled when extrapolating to asteroidal scales, although size-dependent factors (e.g., strain rate) may play an additional role.

Several factors make serpentine an appropriate material for the hydrous projectile and hydrous target. First, serpentine is abundant in C chondrites [22]. Second, the equation of state (EOS) for serpentine is similar to that of C chondrites [23]. Third, CM material is the best analog for OH- and H-bearing dark material on Vesta [26]. Fourth, serpentine is present in impact-delivered dark material on Vesta [25]. Therefore, serpentine is a reasonable analog for the surfaces of carbonaceous asteroids and for the carbonaceous impactors that may ferry water among the asteroids [1].

After impact, pieces of melt breccia were recovered within and near the crater (to ~ 5 crater radii). Geochemistry constrained the fraction of the breccias derived from projectile and target (see [26]). Thermogravimetric analyses (TGA) yielded bulk water contents. Combined, these data constrain how efficiently water can be retained in hydrous projectile and hydrous target experiments. Other techniques provided further information. Micro-scale transmission Fourier transform infrared spectroscopy on doubly-polished sections of the breccias revealed the host of retained water (e.g., impact melt, projectile relics) and speciation (OH vs. H_2O). Powder x-ray diffraction (XRD) on projectile, target, and breccia samples established their mineralogy.

Results: Transmission spectroscopy documented both OH and H_2O in impact glasses (Figure 1). Spectra in Figure 1 were acquired from areas free of projectile relics; the glass itself hosts the OH and H_2O . XRD data yielded insights into serpentine decomposition. Serpentine may decompose to (a) brucite+periclase+stishovite or (b) H_2O +periclase+perovskite [27,28]. Most breccia samples did not show brucite peaks (Fig. 2), a result that favors (b). Assemblage (b) is compatible with earlier planar shock experiments [27] and provides a logical source for water in the glasses. The breccia sample with hints of brucite came from a hydrous target experiment.

Possible kinetic effects [28] may explain such a difference in the products of hydrous projectile and hydrous target impacts.

Implications: These experiments demonstrate that quenched impact melt captures water (OH+H₂O) derived directly from the projectile during impacts into porous, regolith-like targets, consistent with earlier findings [21,29]. Nevertheless, more work is needed to assess whether impact melt or projectile relics constitute the primary reservoir for impact-delivered water at typical main belt speeds of 4.5 to 5 km s⁻¹.

The limited data available for the shock behavior of C chondrites indicate that impact melt plays a key role. Impedance matching calculations using the EOS for Murchison [23] suggest that carbonaceous chondrite impactors completely devolatilize above >3.1 km s⁻¹ (assuming a symmetric impact), if C chondrites completely devolatilize above ~30 GPa as reported by [23]. Only the first contact will experience such conditions, with pressure decaying as 1/r⁻²⁻³. Nevertheless, most impacts in the main belt may partially or completely devolatilize C chondrite-like impactors because 80% of such impacts are >3 km s⁻¹ [15]. The role of thermal decomposition due to frictional shear heating (as seen in carbonates [19]) is not included in such calculations and may enhance devolatilization.

These considerations suggest that OH and H associated with impact-delivered material dark material on Vesta [2,3] is due partly to incompletely devolatilized impactor relics from the lower velocity tail of the impact speed distribution and/or contained in melts generated during typical and higher velocity (e.g., >5 km s⁻¹) impacts. Impacts at 4.5 to 5 km s⁻¹ produce significant melt in regolith analogs [26], which bolsters the case for impact melt as a reservoir. If impact melt successfully traps OH and H during collisions in the main belt (as it does in experiments), then a broader range of impacts may deliver volatiles to Vesta.

Other asteroids also should be laden with significant meteoritic debris as a natural consequence of their impact histories and the impact speeds in the main asteroid belt [26]. Hence, many asteroids—particularly the larger ones—may be plastered with water (OH+H₂O) hosted in partly devolatilized projectile relics and in OH- and H₂O-bearing impact melt produced by the impacts of volatile-rich asteroids and meteoroids.

Figure 1. Transmission spectra of two samples of impact glass. Absorbance peaks at 2.8 and 6.2 μm indicate that both OH and H₂O are present.

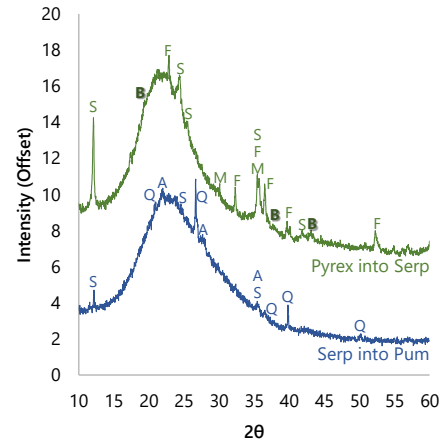
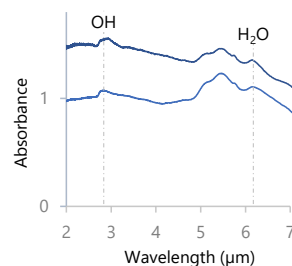


Figure 2. XRD data from samples produced by Pyrex impacting a serpentine target (green) and serpentine impacting powdered pumice (blue). Letters show peak assignments: S=serpentine; Q=quartz; A=anorthite; B=brucite, F=forsterite, M=magnetite. No brucite is seen in the serpentine into pumice sample. Small peaks due to brucite may be present in the Pyrex into serpentine sample. Hence, brucite is not a significant decomposition product, which indicates release of free water. (Some serpentine survived in both experiments.). XRD data show that both samples have abundant glass.

References: [1] Morbidelli et al. (2000) *MAPS*, 35, 1309–1320. [2] Prettyman et al. (2012) *Science*, 338, 242–246. [3] McCord et al. (2012) *Nature*, 491, 83–86. [4] De Sanctis et al. (2012) *ApJ*, 758, L36. [5] Zolensky et al. (1996) *MAPS*, 31, 518–537. [6] Greshake (2014) *MAPS*, 49, 824–841. [7] Krzesinka and Fritz (2014) *MAPS*, 49, 595–610. [8] Downes et al. (2008) *GCA*, 72, 4825–4844. [9] Schultz et al. (2010) *Science*, 330, 468–472. [10] Neumann et al. (2012) *Science*, 339, 296–300. [11] Ong et al. (2010) *Icarus*, 207, 578–589. [12] Bruck Syal and Schultz (2015) *LPS* 46, abstract #1680. [13] Svetsov and Shuvalov (2015) *Planet. Sp. Sci.*, 117, 444–452. [14] Quintana et al. (2015) *LPS* 46, abstract #2727. [15] O’Brien and Sykes (2011) *Sp. Sci. Rev.*, 163, 41–61. [16] Artemieva and Pierazzo (2011) *MAPS*, 46, 805–829. [17] Gault and Wedekind (1978) *LPS IX*, 374–376. [18] Kraus et al. (2013) *JGR*, 118, 2137–2145. [19] Schultz (1996) *JGR*, 101, 21117–21136. [20] Harris and Schultz (2007) *Bridging the Gap II*, abstract #8051. [21] Harris and Schultz (2011) *Wet vs. Dry Moon*, abstract #6042. [22] Howard et al. (2009) *GCA*, 73, 4576–4589. [23] Tyburczy et al. (1986) *EPSL*, 80, 201–207. [24] Palomba et al. (2014) *Icarus*, 240, 58–72. [25] Nathues et al. (2014) *Icarus*, 239, 222–237. [26] Daly and Schultz (2016) *Icarus*, 264, 9–19. [27] Tyburczy et al. (1991) *JGR*, 96, 18011–18027. [28] Zhang et al. (2014) *Phys. Chem. Min.*, 41, 313–322. [29] Harris and Schultz (2015) *LPS* 46, abstract #2585.